Palladium electrodes for molecular tunnel junctions



2012 Nanotechnology 23 425202

(http://iopscience.iop.org/0957-4484/23/42/425202)

Nanotechnology **23** (2012) 425202 (5pp) doi:10.1088/0957-4484/23/42/425202

# Palladium electrodes for molecular tunnel junctions

**Shuai Chang[1], Suman Sen[1,2], Peiming Zhang[1], Brett Gyarfas[1], Brian Ashcroft[1], Steven Lefkowitz[3], Hongbo Peng[4] and Stuart Lindsay[1,2,5]**

[1] Biodesign Institute, Arizona State University, Tempe, AZ 85287, USA
[2] Department of Chemistry and Biochemistry, Arizona State University, Tempe, AZ 85287, USA
[3] 454 Life Sciences, a Roche Company, 20 Commercial Street Branford, CT 06405, USA
[4] IBM TJ Watson Research Center, Yorktown Heights, NY 10598, USA
[5] Department of Physics, Arizona State University, Tempe, AZ 85287, USA

E-mail: Stuart.Lindsay@asu.edu

Received 26 June 2012, in final form 27 August 2012
Published 4 October 2012
Online at stacks.iop.org/Nano/23/425202

**Abstract**
Gold has been the metal of choice for research on molecular tunneling junctions, but it is incompatible with complementary metal–oxide–semiconductor fabrication because it forms deep level traps in silicon. Palladium electrodes do not contaminate silicon, and also give higher tunnel current signals in the molecular tunnel junctions that we have studied. The result is cleaner signals in a recognition-tunneling junction that recognizes the four natural DNA bases as well as 5-methyl cytosine, with no spurious background signals. More than 75% of all the recorded signal peaks indicate the base correctly.

S Online supplementary data available from stacks.iop.org/Nano/23/425202/mmedia

(Some figures may appear in colour only in the online journal)

## 1. Introduction

Gold has been the metal of choice for molecular tunnel junction studies using mechanical break junctions [1], self-assembled junctions [2] or repeated formation of break junctions [3]. This because of the ease of forming monolayers using well-understood thiol chemistry, and also because of the plastic deformation of gold that gives rise to distinct features when junctions are broken [4]. Plasticity of the electrodes is not required for measurements made with fixed junctions [5, 6]. Indeed, such plasticity may even be a disadvantage in terms of the long-term stability of the tunnel junction. From a device standpoint, a more serious concern is that gold forms deep level traps in silicon [7], making it difficult to integrate gold tunnel junctions with complementary metal–oxide–semiconductor (CMOS) electronics. Aware of this problem, the Whitesides laboratory showed that thiol attachment chemistry works well on palladium surfaces [8] so the same types of molecule can be studied in either gold or palladium junctions. In addition, a theoretical calculation suggests that palladium electrodes might give bigger signals than gold electrodes. Lawson and Bauschlicher [9] calculated the conductance of a phenoldithiol molecule spanning pairs of gold, silver, platinum and palladium electrodes, finding that platinum and palladium gave substantially higher calculated tunnel conductance than gold. Thus, in addition to its CMOS compatibility, palladium may also make a better electrode material. Palladium surfaces do not form the large 111 flat terraces that are readily found on gold, so they are a little harder to study. Nonetheless, we have found that STM probes and substrates are readily fabricated and easily functionalized with thiolated molecules.

We tested palladium electrodes for recognition tunneling, a technique developed to read single nucleo-bases for DNA sequencing applications [10]. In recognition tunneling, each electrode in the gap is functionalized with adaptor molecules that make non-covalent bonds with an analyte that enters the tunnel gap (figure 1(A)). The adaptor molecules make a more specific set of chemical contacts with the target than bare metal electrodes would, and they also reduce the problem

 

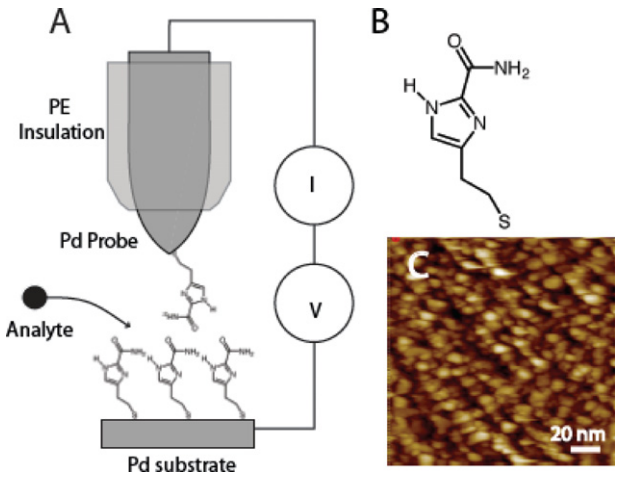


**Figure 1.** Recognition tunneling with Pd electrodes. (A) A Pd covered Si wafer is functionalized with a monolayer of an imidazole-carboxamide molecule (B) as is the end of an electrochemically etched Pd wire. The wire is insulated with polyethylene, leaving a fraction of a square micron of exposed area. The junction is submerged in buffered aqueous electrolyte containing analyte molecules that diffuse into the tunnel junction. (C) STM image of a Pd coated substrate showing 10 nm grains.

of contamination on the electrode surfaces, because of the lower surface energy of the modified surface and displacement of hydrocarbons via the metal–thiol interaction. Enhanced tunneling through the adaptor molecules (which have a smaller HOMO–LUMO gap than water molecules) means that tunnel gaps can be quite large, easily accommodating a nucleotide [11]. The trapped analyte generates a stochastic train of tunnel current pulses which can be used to identify the analyte through its characteristic 'fingerprint' as analyzed by a machine-learning algorithm called a support vector machine [12, 13].

We formed junctions functionalized with a thiolated imidazole-carboxamide molecule (figure 1(B)) recently introduced as a 'universal reader' for DNA bases [12, 14]. The tunneling geometry is shown in figure 1(A). We obtained signals from all four bases (and 5-methylcytosine) at smaller tunnel conductances than were required for obtaining such data from a gold junction. In consequence, the signals were free of an interfering background signal found with gold electrodes [12], and better separation of the amplitude signals was obtained.

## 2. Experimental methods

We made Pd substrates on a 750 $\mu$m silicon wafer using e-beam evaporation of 100 nm of Pd onto a 10 nm Ti adhesion layer. The grain size, measured by STM imaging, was about 10 nm (figure 1(C)). Probes were etched from 0.25 mm Pd wire (California Fine Wires) using the procedures described for making gold probes earlier [15], except that a higher peak to peak voltage (40 V rather than 30 V) was used for the first stage. The probes were insulated with polyethylene to leave the metal end open with a linear dimension a few tens of nm. The procedure was identical to that used for gold probes, except that the yield was a little higher because the palladium is harder.

Pd substrates [16] were annealed with a hydrogen flame for 30–40 s and then immediately immersed in a 0.5 mM ethanol solution of 4(5)-(2-mercaptoethyl)-1H-imidazole-2-carboxamide [14], where they were left for a minimum of 18 h, then rinsed in ethanol and then blown dry with nitrogen before immersing them in the phosphate buffer solution. The resulting monolayers were characterized by XPS, contact angle measurements, ellipsometry and FTIR as described in the supplementary information (figures S1–S4 and table S1, supporting information available at stacks.iop.org/Nano/23/425202/mmedia). Insulated probes were cleaned prior to functionalization by rinsing them with ethanol and $H_2O$, drying them in nitrogen, and then immersing them in a 0.5 mM solution of 4(5)-(2-mercaptoethyl)-1H-imidazole-2-carboxamide [14] in ethanol for 3 h. There is no tool equivalent to XPS or FTIR for testing functionalization of a probe. We were able to test the efficiency of the functionalization process by making recognition-tunneling measurements on a functionalized Pd surface, and comparing the tunneling data to controls in which the probe was functionalized, but the substrate was left bare. The resulting tunneling signals showed clearly whether or not functionalization was successful (figures S5 and S6, supporting information available at stacks.iop.org/Nano/23/425202/mmedia). Nucleotide 5′-monophosphates were purchased from Sigma-Aldrich, and used without further purification. They were dissolved to a final concentration of 10 $\mu$M in 1 mM phosphate buffer. All solutions were prepared using Nanopure water.

Tunneling measurements were carried out in phosphate buffered aqueous solutions using a picoSPM (Agilent, Chandler, AZ) with a Teflon liquid cell that was rigorously cleaned between measurements.

## 3. Results and discussion

Current versus time traces are shown for a control sample (1 mM phosphate buffer, pH = 7) and the five nucleotides in figure 2. These data were obtained at a probe bias of 0.5 V at a set-point tunnel current of 2 pA. The control signal is completely free of features. The four nucleo-bases and deoxy-5-methylCMP produce characteristic recognition-tunneling signal spikes. This result stands in contrast to gold electrodes, where the set-point tunnel current has to be increased to 6 pA before signals are observed from all the bases, with the added drawback that spurious signals are observed in buffer solution alone at this higher conductance set-point [12].

The distribution of measured peak heights at a set-point of 2 pA and 0.5 V is shown in figure 3(A) for the Pd electrodes. For comparison, distributions measured for gold electrodes at a set-point of 6 pA and 0.5 V are shown in figure 3(B) (these data are unfiltered so differ from earlier published data as explained in the figure caption). The differences are most striking for dGMP where many peak current levels exceed 50 pA, at a set-point conductance where no data is

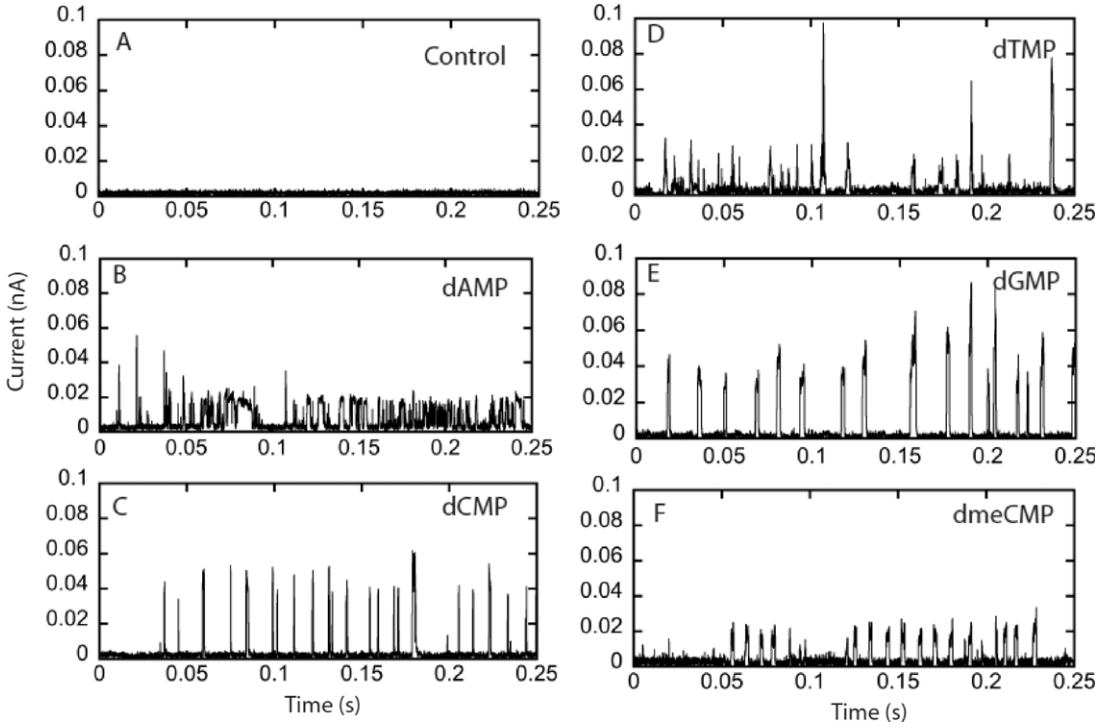


**Figure 2.** Characteristic signals obtained at a set-point current of 2 pA and a bias of 0.5 V for (A) 1 mM phosphate buffer alone. The control is free of the small features generated using gold electrodes (at the higher set-point required to generate nucleotide signals with gold electrodes). The remaining panels show signals for (B) dAMP, (C) dCMP, (D) dTMP, (E) dGMP and (F) $d^{5me}$ CMP in the same tunneling conditions, all at 10 $\mu$M concentration in 1 mM phosphate buffer, pH 7.0. The dAMP signals illustrate the stochastic nature of recognition-tunneling signals, being composed of both large spikes and smaller amplitude telegraph noise. All parts of the signal are used for training the recognition algorithm.

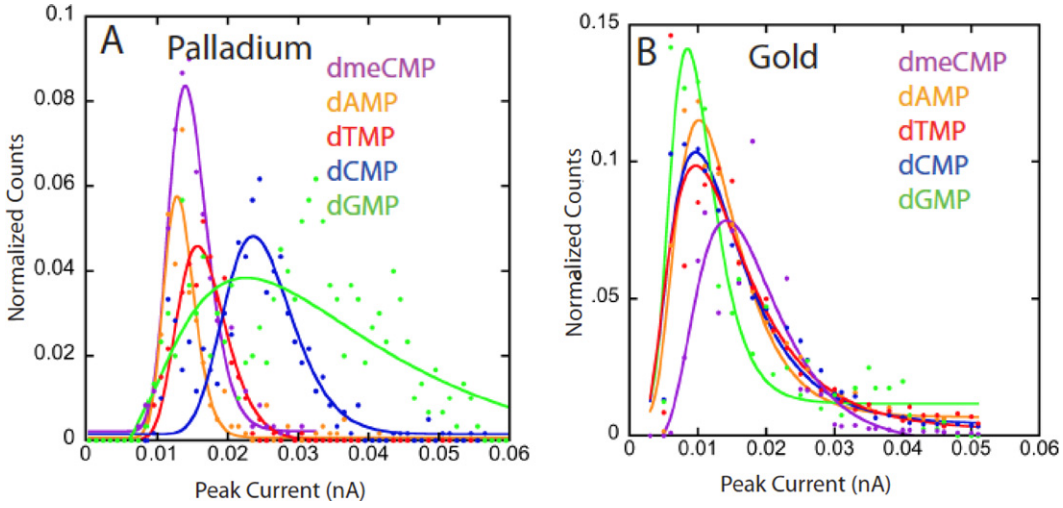


**Figure 3.** Distribution of peak spike intensities for (A) Pd electrodes operated at 2 pA and 0.5 V and (B) Au electrodes operated at 6 pA and 0.5 V. The data are somewhat better separated by the Pd electrodes, and peak currents are larger, despite the significantly smaller operating conductance of the Pd junction. Histograms are compiled for each of the five nucleoside monophosphates as labeled. Solid lines are fits to log-normal distributions with peak positions as listed in table 1. The amplitude distributions shown here for gold electrodes differ from those previously published [12] because we have not filtered the data shown here, except to remove small water peaks from the distribution.

recorded at all with gold electrodes. Even at the threefold higher conductance (12 pS versus 4 pS) used to obtain data with gold electrodes, few peak currents exceeded 20 pA. For gold electrodes, the amplitude distributions for all 5 bases are almost completely overlapped (an additional overlapping water contribution had been removed). It was possible to obtain some amplitude selectivity by filtering for a particular pulse shape, but this resulted in rejection of a large fraction of the data [12]. In contrast, signals obtained with Pd electrodes (a) require no filtering to remove a background signal and (b)

show some amplitude separation with no selection applied to the data at all. We speculate that this is a consequence of the larger tunnel gap obtained at the lower conductance set-point. This increases the contribution of the molecular complex in the gap to the tunnel conductance relative to the effects of contact geometry [17].

The broad distribution of spike amplitudes makes base calling based on amplitudes alone almost impossible. However, many other features of the signal stream convey specific chemical information. Among these are the pulse shapes (as characterized by Fourier and wavelet components), the pulse widths, pulse frequencies, distribution of pulses in a cluster and so on. In an earlier paper, we showed how a multidimensional parameter space can be constructed such that data from each of the bases can be optimally partitioned, allowing base calling with quite high accuracy even on one single molecule read [12, 13]. Recognition-tunneling data tend to occur in clusters where repeated signals are generated by the same base trapped in the tunnel junction [10]. We have written an algorithm that automatically locates such clusters (described in Chang *et al* [12]) and the distribution of pulses within a cluster was analyzed both with Fourier coefficients and wavelet components. An optimum combination of parameters is found by taking random selections of the various parameters, training a support vector machine, and then testing it on known data. The combination of parameters that yields the highest true-positive rate of calling signal spikes is retained, together with the accompanying support vectors. Each spike in the data stream can be used to call a base once this data is available. In the case of gold electrodes the true-positive rate is about 80% once a (substantial) amount of water background is removed. We applied the same analysis to the data obtained from Pd electrodes, only in this case no data was removed by prefiltering. The only two parameters that required adjustment were: (1) The threshold above a background above which a peak was called. This was set to 8 pA above the 2 pA baseline. (2) The value above the baseline to which a current must drop to be considered in the baseline. This was set to 3 pA. Peaks below 8 pA in height contained no specific information while the 3 pA lower threshold was high enough above the background that the end of a peak was readily determined. With the parameter combination listed in table S2 (supporting online information available at stacks.iop.org/Nano/23/425202/mmedia) more than 75% of the peaks call the correct base. The distribution of correct calls among the five bases is listed in table 1. The calling accuracy is likely to be higher than the true-positive rate, because there are many repeated reads on each nucleotide. However, our current version of the SVM code does not assign probabilities in a way that allows this calculation to be carried out.

The excellent signal levels (figure 2) suggest that operation may be possible at lower bias, an important consideration for a nanopore-based sequence reader where the electric field used for readout could interfere with the electric field used to drive translocation through the pore. We obtained an excellent count rate for a dTMP target at a bias of 0.1 V and a set-point current of 4 pA (figure S7(A), supporting online information available at stacks.iop.org/Nano/23/425202/mmedia). Controls taken with buffered electrolyte alone were clean in these conditions (figure S7(B), supporting online information available at stacks.iop.org/Nano/23/425202/mmedia).

**Table 1.** Frequency of single signal spikes that call a base correctly for data obtained with Pd electrodes. Also listed are the peaks of the current distributions for Pd and Au electrodes. The number of peaks analyzed reflects different signal generation rates for the five nucleotides. The analysis used every recorded signal spike with no data rejection.

| Nucleotide | Number of peaks analyzed | True-positive rate (%) | Peak current pA (Pd) | Peak current pA (Au) |
|---|---|---|---|---|
| dAMP | 1698 | 81 | $13.1 \pm 0.1$ | $12.3 \pm 0.4$ |
| dCMP | 2594 | 76 | $24.6 \pm 0.3$ | $12.0 \pm 0.7$ |
| dGMP | 4567 | 82 | $33.3 \pm 3$ | $9.7 \pm 0.4$ |
| dTMP | 1428 | 83 | $16.4 \pm 0.1$ | $13.5 \pm 1.5$ |
| $d^{me}CMP$ | 5013 | 78 | $14.1 \pm 0.1$ | $16.9 \pm 0.1$ |

In earlier work [12], we found that when the tunnel junction was presented with mixtures of nucleotides, the support vector machine found many signals that it could not recognize based on its training with a pure solution of just one nucleotide, presumably because of interactions between the different nucleotides. We synthesized a 5′-AG-3′ dimer (supporting information available at stacks.iop.org/Nano/23/425202/mmedia) reasoning that the phosphodiester backbone would keep the nucleotides apart and minimize inter-strand interactions. We measured the tunneling signals from a 5 $\mu$M solution in 1 mM phosphate buffer (pH 7.0). An example of a recording is shown in figure S8 (supporting information available at stacks.iop.org/Nano/23/425202/mmedia) showing a transition from G-like signals to A-like signals (cf, figure 2). Using the support vectors generated by the individual nucleotides, together with the optimum parameter set from those experiments, the SVM called 57% of the peaks as G, 30% as A, 10% as C and 3% as T. This is a substantial improvement on the calling accuracy obtained with nucleotide mixtures. There are a significant number of erroneous C calls suggesting that there are significant differences between nucleotides within polymers and individual nucleotides. In a sequencing application the SVM should be trained on hompolymers rather than isolated nucleotides.

In conclusion, recognition tunnel junctions are readily assembled using Pd electrodes. Functionalized with 1H-imidazole-2-carboxamide adaptor molecules and operated at a gap conductance of 4 pS ($V = 0.5$ V, $i = 2$ pA) they give no spurious signals from a buffered aqueous electrolyte alone, but produce tunneling signals from all five DNA bases. Operation at a bias as low as 0.1 V is possible, at least for the dTMP tested. Each peak in the signal train is assigned to the correct base 80% of the time. If the signal peaks are generated independently, the overall read accuracy may be higher than 80%, but a calculation awaits a version of the SVM code that generates useful probabilities on each call.

## Acknowledgments

This work was funded by grants from the DNA sequencing technology program of the NIH (R01 HG006323 and R21 HG005851) and a sponsored research agreement with Roche/454 Life Sciences. We thank Tim Karcher of the Leroy Eyring Center for Solid State Science for carrying out the XPS analysis and Shuhui Wu of the Center for Single Molecule Biophysics for synthesizing the AG dimer.

## References

[1] Reed M A, Zhou C, Muller C J, Burgin T P and Tour J M 1997 Conductance of a molecular junction *Science* **278** 252–4

[2] Cui X D, Primak A, Zarate X, Tomfohr J, Sankey O F, Moore A L, Moore T A, Gust D, Harris G and Lindsay S M 2001 Reproducible measurement of single-molecule conductivity *Science* **294** 571–4

[3] Xu B and Tao N J 2003 Measurement of single-molecule resistance by repeated formation of molecular junctions *Science* **301** 1221–3

[4] Van Ruitenbeek J M 2000 Experiments on conductance at the atomic scale *Quantum Mesoscopic Phenomena and Mesoscopic Devices in Microelectronics* (Berlin: Springer) pp 35–50

[5] Haiss W, Nichols R J, Zalinge H v, Higgins S J, Bethell D and Schiffrin D J 2004 Measurement of single molecule conductivity using the spontaneous formation of molecular wires *Phys. Chem. Chem. Phys.* **6** 4330–7

[6] Lindsay S, He J, Sankey O, Hapala P, Jelinek P, Zhang P, Chang S and Huang S 2010 Recognition tunneling *Nanotechnology* **21** 262001

[7] Tavendale A J and Pearton S J 1983 Deep-level quenched-in defects in silicon doped with gold, silver, iron, copper or nickel *J. Phys.: Condens. Matter* **16** 1665–73

[8] Love J C, Wolfe D B, Chabinyc M L, Paul K E and Whitesides G M 2002 Self-assembled monolayers of alkanethiolates on palladium are good etch resists *J. Am. Chem. Soc.* **124** 1576–7

[9] Lawson J W and Bauschlicher C W 2006 Transport in molecular junctions with different molecular contacts *Phys. Rev.* B **74** 125401

[10] Huang S, He J, Chang S, Zhang P, Liang F, Li S, Tuchband M, Fuhrman A, Ros R and Lindsay S M 2010 Identifying single bases in a DNA oligomer with electron tunneling *Nature Nanotechnol.* **5** 868–73

[11] Chang S, He J, Zhang P, Gyarfas B and Lindsay S 2011 Analysis of interactions in a molecular tunnel junction *J. Am. Chem. Soc.* **133** 14267–9

[12] Chang S *et al* 2012 Chemical recognition and binding kinetics in a functionalized tunnel junction *Nanotechnology* **23** 235101

[13] Chang C-C and Lin C-J 2011 LIBSVM: a library for support vector machines *ACM Trans. Intell. Syst. Technol.* **2** 27–52

[14] Liang F, Li S, Lindsay S and Zhang P 2012 Synthesis, physicochemical properties, and hydrogen bonding of 4 (5)-substituted-1H-imidazole-2-carboxamide, a potential universal reader for DNA sequencing by recognition tunneling *Chem.—Eur. J.* **18** 5998–6007

[15] Tuchband M, He J, Huang S and Lindsay S 2012 Insulated gold scanning tunneling microscopy probes for recognition tunneling in an aqueous environment *Rev. Sci. Instrum.* **83** 015102

[16] DeRose J A, Lampner D B and Lindsay S M 1993 A comparative SPM study of the surface morphology of Au films grown from the vapor onto glass, fused silica and muscovite mica *J. Vac. Sci. Technol.* **A11** 776–80

[17] He J, Sankey O F, Lee M, Tao N J, Li X and Lindsay S M 2006 Measuring single molecule conductance with break junctions *Faraday Discuss.* **131** 145–54